IEEE Access
Multidisciplinary | Rapid Review | Open Access Journal

Received September 21, 2020, accepted November 1, 2020, date of publication November 16, 2020,
date of current version November 24, 2020.

Digital Object Identifier 10.1109/ACCESS.2020.3038004

Electromagnetic Biological Effect on Mice in Wireless Power Transmission System

JUN ZHAO[1,2], ZHIJUN WU[1,2], TING YANG[1,2], YIHANG ZHAO[1,2], AND LEI WANG[3]

[1]State Key Laboratory of Reliable and Intelligence of Electrical Equipment, Hebei University of Technology, Tianjin 300130, China
[2]Tianjin Key Laboratory of Bioelectromagnetic Technology and Intelligent Health, Hebei University of Technology, Tianjin 300130, China
[3]Institute of Biomedical Engineering, Chinese Academy of Medical Sciences and Peking Union Medical College, Tianjin 300192, China

Corresponding author: Lei Wang (leiwang2006163@163.com)

This work was supported in part by the National Natural Science Foundation of China under Grant 51407058.

ABSTRACT In this paper, the wireless power transmission system and the model of mouse with its main organs are established to simulate the electromagnetic field and electromagnetic thermal effect. The mouse is placed at the system, and the peak value of the induced electric field intensity and temperature rise of each organ are calculated. The results show that the peak value of the induced electric field intensity of the liver is the largest, which is 1.43 V/m. Temperature rise of the kidney is the largest, which is 2.736×10^{-6}°C. And the results indicate that the shielding plate can effectively reduce the peak value of induced electric field intensity and temperature rise of the main organs. Then, a biosafety experimental platform for the wireless power transmission system is set up to analyze changes in biological tissue structure, immune factors, and sex hormone content. The results show that the level of immune factors in mice increase significantly, and the level of testosterone and progesterone decrease. The heart tissue structure does not change, but the liver, spleen, ovary, and testes are affected. And the liver shows the greatest morphological changes, which is consistent with the simulation results. This study provides a theoretical basis for the security assessment of the wireless power transmission system.

INDEX TERMS Wireless power transmission, finite element analysis, electromagnetic exposure, biosafety.

I. INTRODUCTION

Since the discovery and application of electrical energy, it has changed people's production and lifestyle and has become one of the important energy sources that people rely on. Wireless power transmission (WPT) is a technology that transmits energy through the physical electromagnetic field, and it is a focus in the market, such as implantable biomedical devices, electric vehicles, electric bicycles, mobile devices, and household appliances [1]–[4].

In 2007, WPT shocked the world when an MIT research team led by Marin Soljacic transmitted 60 watts of power over 2 meters wirelessly and the efficiency was 40% [5]. However, while WPT technology brings convenience to people's lives, the effect of electromagnetic fields (EMF) generated by WPT systems on organisms should also be considered. Carpenter's research indicates that excessive exposure to magnetic fields from power lines and other sources of electric current increases the risk of development of some cancers and neurodegenerative diseases, and that excessive exposure to radiofrequency radiation increases the risk of cancer, male infertility, and neurobehavioral abnormalities [6]. The EMF from WPT system has been evaluated in basic dosimetry studies using human body models [7]–[14]. Some studies have shown that magnetic fields had an association with the risk of childhood leukemia [15]–[17]. The effect of EMF on the immune function of organisms has also been studied [18]. The biological safety of EMF exposure has received increasing international attention, so further research is needed. The objective of this paper is to use a combination of simulation calculation and biological experiments to analyze the electromagnetic biological effects of the WPT system on mice by calculating the electromagnetic field distribution and detecting changes in biological parameters in mice.

In this paper, a model of the WPT system and a mouse with its main organs are established to calculate the peak values of induced electric field intensity and temperature changes of the main organs of the mouse by COMSOL 5.0. Then, a WPT system biosafety experimental platform is set up to analyze the changes of organ tissue structure, immune factor, and

The associate editor coordinating the review of this manuscript and approving it for publication was Utku Kose.

sex hormone when mice are exposed to the system. And the simulation data and experimental results are combined to analyze the effects of the WPT system on mice, which provided some theoretical basis for the research on the biological safety of the WPT system.

II. MODELING AND SIMULATION OF THE WPT SYSTEM

A. MODELING OF THE WPT SYSTEM AND MOUSE

The transmitting and receiving coils of the WPT system established in this paper are equipped with a magnetic shielding plate made of a ferrite material with the relative permeability of 2500 and the conductivity of 1. Since the current-carrying capacity of the coil is limited when it is working, and there is skin effect and its own inductance, the parameters used in this paper after comprehensively considering the above factors are shown in Table 1. Among them, the inductance and capacitance follow the resonance condition:

$$X = \omega L - \frac{1}{\omega C} = 0 \tag{1}$$

where $\omega = 2\pi f, f = 47kHz$.

TABLE 1. Resonator parameters.

Parameters	Value
Frequency (kHz)	47
Internal dimensions (m)	0.24×0.24
Outside dimensions (m)	0.4×0.4
Magnetic shield plate size (m)	0.4×0.4×0.01
Distance between two coils (m)	0.2
Coil inductance (μH)	84.542
Compensation capacitor (nF)	135.635
Number of turns (n)	10
Efficiency (%)	97.439

The maximum transmission efficiency of the system at different frequencies is determined by adjusting the load resistance. The transmission efficiency can be given by (2).

$$|\eta| = \frac{|I_o^2 \cdot R|}{|U_s \cdot I_{in}|} \tag{2}$$

where I_o is the output current,R is the load resistance, U_s is the input voltage, and I_{in} is the input current.

The resonance frequency of the system is controlled through an external matching capacitor. The structure of the coils on both sides is completely symmetrical. The schematic diagram of the resonant coil model is shown in Figure 1.

To analyze the effect on a mouse in the WPT system, CT data of a three-month-old healthy Kunming mouse are used to establish the model of a mouse and its main organs through reverse engineering. The main process includes setting the gray threshold, segmentation by region growth, smoothing the target area, and split the model. Due to the limited resolution of CT data, the testes and ovaries of the mouse cannot be distinguished accurately, so spheres are used instead. The model of mouse and its split results are shown in Figure 2.

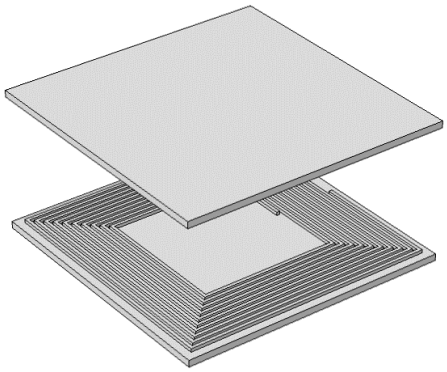

FIGURE 1. Schematic diagram of resonant coil model.

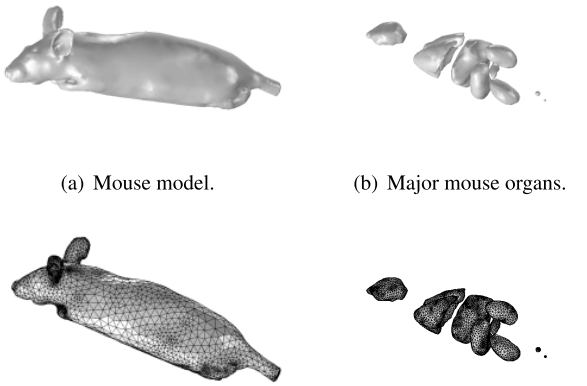

(a) Mouse model. (b) Major mouse organs.

(c) Mouse split result . (d) Major organs split result.

FIGURE 2. Mouse model and its split results.

When a time-varying electric field is applied, biological tissue can be regarded as a linear and isotropic medium, and the tissue conductivity will change with the change of frequency. Studies have shown that almost all biological tissues can be regarded as non-magnetic tissues, and their permeability $\mu = \mu_0$ (or relative permeability $\mu_r = 1$). According to the research results of related literature [19], the electromagnetic parameters of the main organs of mice at 47 kHz are shown in Table 2.

TABLE 2. Mouse organ electromagnetic parameters at 47KHZ.

Organs	Permittivity	Conductivity(S/m)
Brain	4730.25	0.10212
Lung	6716.45	0.18171
Heart	17872	0.19378
Liver	11056	0.071158
Kidney	11891	0.1585
Stomach	3635.9	0.53352
Spleen	5644.3	0.11756
Ovary	3137.8	0.33589
Testis	6575.1	0.43415

B. SIMULATION OF ELECTROMAGNETIC FIELD OF THE WPT SYSTEM

The WPT system constructed in this paper has a working frequency of 47kHz and an output power of 30W, which is suitable for the power supply of household appliances. The field-circuit coupling model of the WPT system is shown in Figure 3.

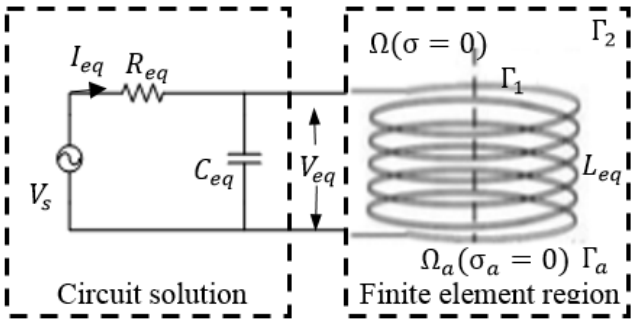

FIGURE 3. Field-circuit coupling diagram of WPT system.

In Figure 3, V_s is the high-frequency power supply, V_{eq}, I_{eq}, and R_{eq} are the equivalent voltage, current and resistance of the coil at high frequency, L_{eq} is the equivalent inductance of the coil, C_{eq} is the equivalent capacitance. Ω_a and Γ_a represent the resonator region and boundary, respectively, Ω, Γ_1, and Γ_2 respectively represent the non-resonator region and its boundary, and σ is the conductivity of the solution region. And the numerical calculation of the electromagnetic field region is resolved by the finite element method.

When the system is working, both electric and magnetic fields satisfy Maxwell's equations, and the finite element area satisfies the following relationship:

$$\begin{cases} \Omega : \begin{cases} \nabla \times \boldsymbol{H} = \sigma \boldsymbol{E} \\ \nabla \times \boldsymbol{H} + j\omega \boldsymbol{B} = 0 \\ \nabla \cdot \boldsymbol{B} = 0 \end{cases} \\ \Gamma_1, \Gamma_2 : \boldsymbol{n} \cdot \boldsymbol{B} = 0 \\ \Omega_a : \begin{cases} \nabla \times \boldsymbol{H}_a = \boldsymbol{\sigma}_a \boldsymbol{E}_a + \boldsymbol{J}_s \\ \nabla \cdot \boldsymbol{B}_a = 0 \end{cases} \\ \Gamma_a : \begin{cases} \boldsymbol{n}_a \times (\boldsymbol{E} - \boldsymbol{E}_a) = 0 \\ \boldsymbol{n}_a \cdot (\boldsymbol{B} - \boldsymbol{B}_a) = 0 \end{cases} \end{cases} \tag{3}$$

In the formula, $\boldsymbol{H}$ is the magnetic field strength; $\boldsymbol{E}$ is the electric field strength; $\boldsymbol{B}$ is the magnetic flux density vector; $\boldsymbol{J}_s$ is the source current density; ω is the system angular frequency; $\boldsymbol{n}$ is the boundary normal vector. The expression with subscript a is the value at the resonator area and boundary. The voltage constraint equation of the circuit solution area is:

$$V_s + I_{eq} R_{eq} = V_{eq} \tag{4}$$

In order to observe and analyze the electromagnetic field environment of the WPT system visually, at the center point of the resonance coil, we make a cut plane perpendicular to the resonance coil, and calculate the electromagnetic field distribution on the cut plane in COMSOL 5.0. The magnetic induction intensity distribution is shown in Figure 4(a), and the electric field intensity distribution is shown in Figure 4(b). We also make a cross-section parallel to the coil with a distance from the center of the two coils (100 mm in the Z-axis direction), and calculate the magnetic induction intensity distribution on the plane. The result is shown in Figure 5.

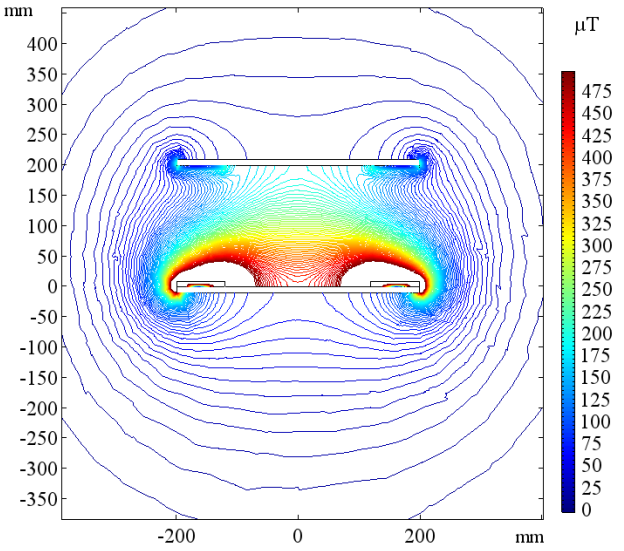

(a) Magnetic induction intensity.

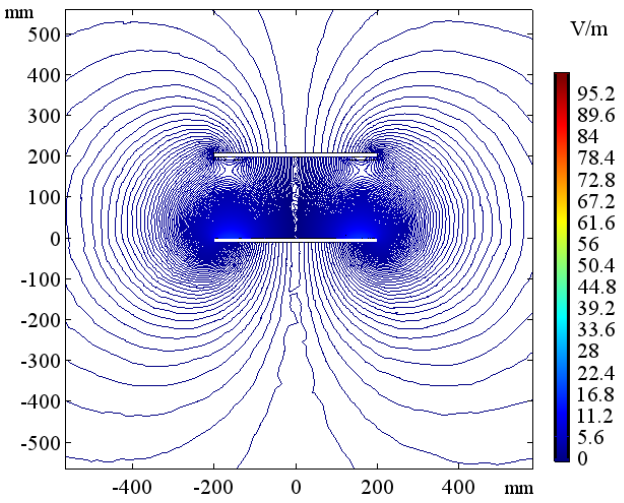

(b) Electric field intensity.

FIGURE 4. Mouse model and its split results.

It can be seen from Fig. 5 that the X-axis and Y-axis are position coordinates of the cross-section, and the Z-axis is the magnetic induction intensity value. The magnetic induction intensity at the center of the coil is the largest on the same plane.

C. EFFECTS OF THE WPT SYSTEM ON MAIN ORGANS OF MOUSE

Based on the analysis above, during the simulation, the mouse is placed in the center of the coils, as shown in Figure 6.

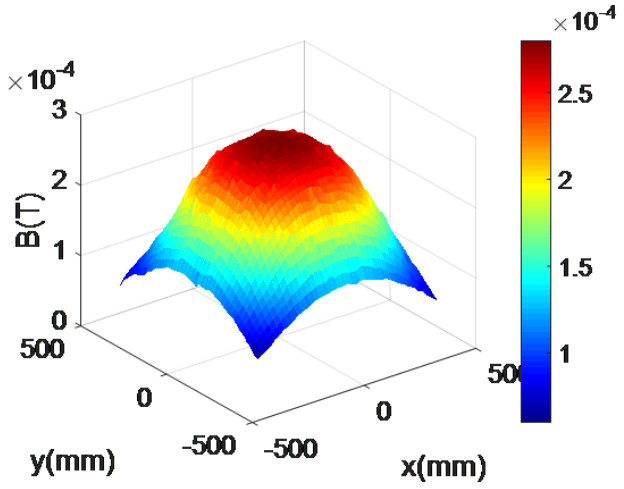

FIGURE 5. Cross-section magnetic induction intensity distribution.

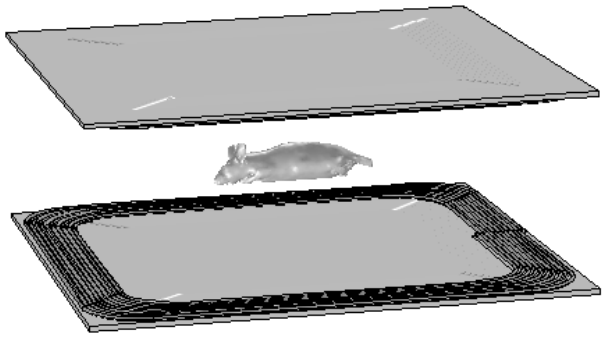

FIGURE 6. Schematic diagram of resonant coil model.

The effect of exposure to EMF depends on its frequency and intensity or magnitude. When the mouse is in the system, the mouse's body perturbs the electrical field but not the magnetic field, and therefore, the internal and external magnetic field are approximate equal, as shown in Figure 7.

Therefore, a magnetic field generates an induced internal electrical field referring to Maxwell–Faradays' Equation $\nabla \times \boldsymbol{E} = -\frac{\partial \boldsymbol{B}}{\partial t}$.

In the standard issued by the International Commission on Non-Ionizing Radiation Protection (ICNIRP), the physical quantity used to specify the basic restriction of electromagnetic field exposure is the intensity of the electric field in the body, which is because the electric field will have a greater impact on nerve cells and other electrically sensitive cells [20].

The biological heat transfer in this article is described by Penne's bio-heat equations which is written as:

$$\rho c \frac{dT}{dt} = \nabla(k \nabla T) + \omega_b c_b (T_a - T) + q_m \tag{5}$$

where ρ is the mass density, c is the specific heat capacity, k is the thermal conductivity, and q_m is the metabolic heating. c_b, ω_b, T_a are the specific heat capacity, perfusion rate, and

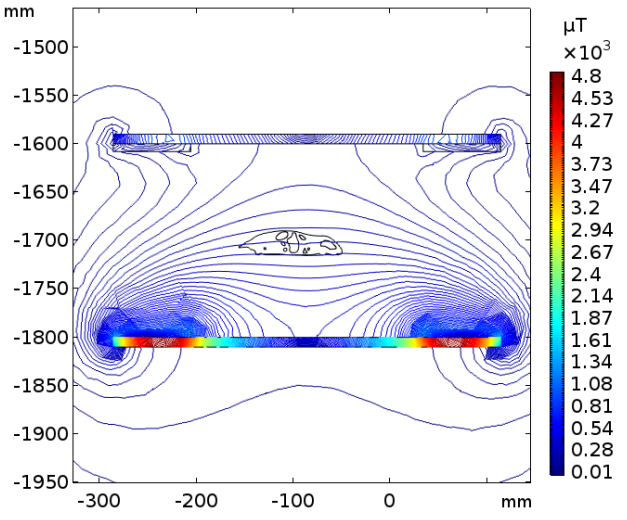

(a) Magnetic induction distribution map.

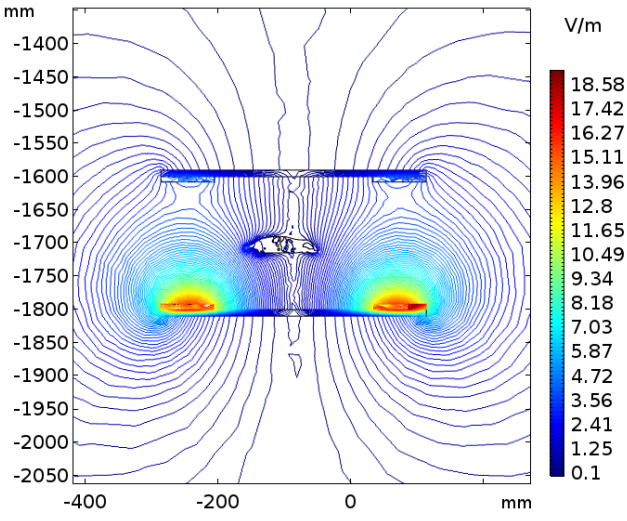

(b) Electric field intensity distribution map.

FIGURE 7. Results of interference of the mouse on electromagnetic field.

temperature of the blood, respectively. T is the temperature to be targeted.

Therefore, this paper calculates the peak values of induced electric field intensity and temperature changes in the main organs of mouse. Because the basic restrictions do not include Specific Absorption Rate (SAR) at frequencies below 100 kHz, simulation calculation for SAR is not included at 47 kHz. The calculation results are shown in Table 3.

It can be seen from Table 3 that the peak values of induced electric field intensity in the liver and kidney are higher than that of other organs, which are due to the different electromagnetic parameters, shapes, and electromagnetic environment of different organs. But all the results are lower than the safety standards issued by ICNIRP, which is 6.345 V/m. According to the results of cell and animal experiments, ICNIRP has found that when tissue temperature rises below 1 °C, no adverse effects on animal tissues are found. From the calculation results, the temperature of the

TABLE 3. Calculation results of mice organs.

Organs	Peak values of induced electric field intensity(V/m)	Temperature rise(10^{-6} °C)
Brain	0.80649	1.2249
Lung	0.97381	2.5486
Heart	0.80243	2.1853
Liver	1.43040	2.6953
Kidney	1.18650	2.7366
Stomach	0.52082	2.4669
Spleen	0.71230	1.8960
Ovary	0.21739	1.1136
Testis	0.21784	1.1071

liver, kidney, lung, and stomach increased greatly, but the values are all within the safety limit. The calculation results are shown in Figure 8.

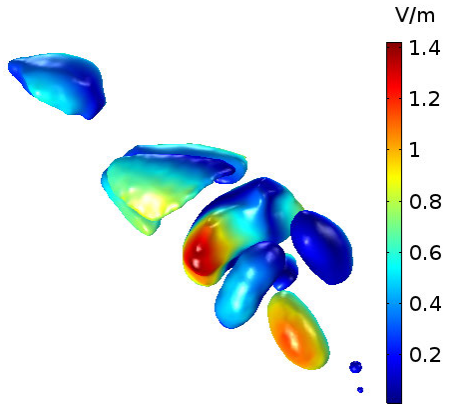

(a) Peak value of induced electric field intensity.

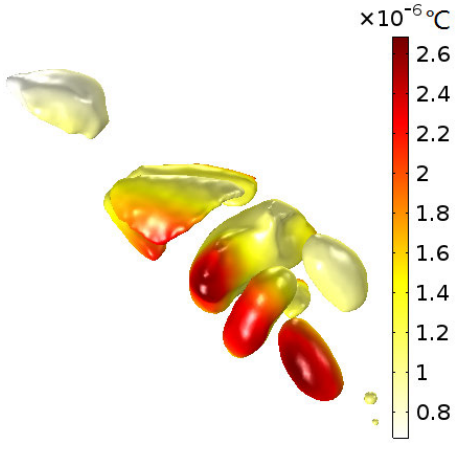

(b) Temperature rise.

FIGURE 8. Distribution of calculation results in main organs of mice.

In order to analyze the effects of electromagnetic fields on mice, the equivalent section of the induced electric field intensity of the mouse organs are calculated, and the distribution of the maximum value of the induced electric field intensity can be clearly observed. The result is shown in Figure 9.

It can be seen from Figure 9 that the induced electric field intensity is attenuated to a very small value at a location far away from the mouse epidermis, and the maximum value occurs near the epidermis.

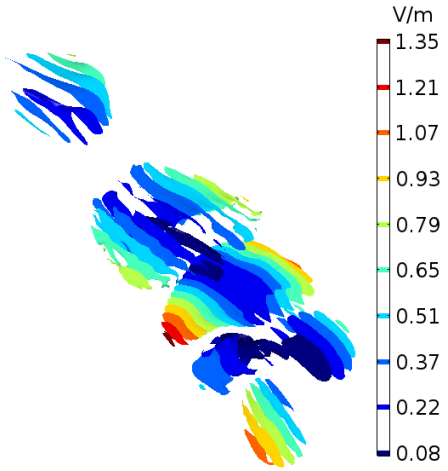

FIGURE 9. The equivalent section of the induced electric field intensity of the mouse organs.

The two different cases of the mouse in the system position a (as shown in Figure 10 (a)) and position b (as shown in Figure 10 (b)) are also simulated.

The peak values of induced electric field intensity and temperature rise of different organs in the mouse are simulated and calculated. The results are shown in Figure 11.

As shown in Figure 11, the peak value of the induced electric field intensity and the temperature rise when the mouse is located at the position b are lower than those when the mouse is located at the position a. This is because the magnetic induction intensity at the position b is lower, which indicates that the shielding plate can be added to effectively reduce the peak value of induced electric field intensity and organ temperature rise of the main organs.

III. CONSTRUCTION OF THE WPT SYSTEM AND EXPERIMENT

A biosafety experimental platform for the WPT system is set up to analyze the effect on mice in system. Some studies have shown that different EMF can cause damage to different organs and immune function [21]–[24]. Therefore, the organ structure, immune factors, and sex hormones are studied in this paper.

The life cycle of mice is short, one month to three months old is the most sensitive period of radiation. So twenty one-month-old healthy KM mice were divided into four groups randomly: group *a* was the control group with

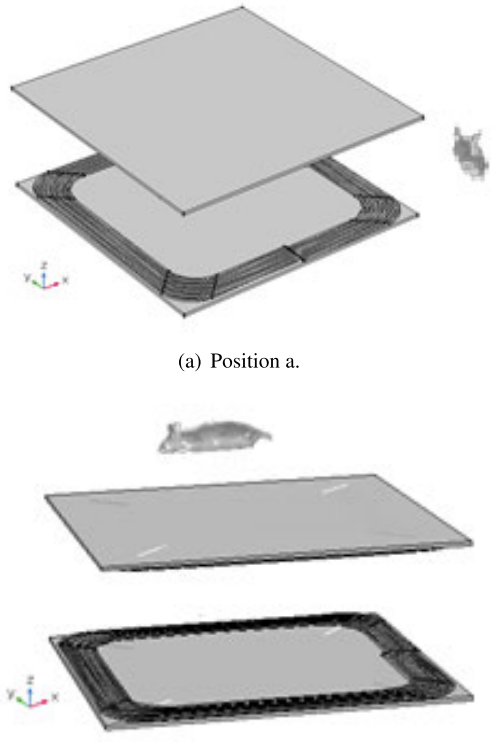

(a) Position a.

(b) Position b.

FIGURE 10. Simulation diagram of mouse at different positions of the resonance coil.

five female mice, group *b* was the experimental group with five female mice, group *c* was the control group with five male mice, and group *d* was the experimental group with five male mice. The average magnetic induction intensity of the activity range of mice was 270μT, which was consistent with the simulation conditions. The mice were purchased from Vital River Laboratories, and the certificate number is SCXK9 (Beijing) 2016-0006. This experiment has passed the review of the Biomedical Ethics Committee of Hebei University of Technology. The ethical review number is HEBUTaCUC2019003. All research was performed in accordance with the relevant guidelines and regulations. The biosafety experimental platform is shown in Figure 12.

During the experiment, the mice in the experimental group were exposed in the WPT system for 5 hours a day, 6 days a week regularly. They were supplied with food and water as usual. The mice in the control group were fed in a normal environment routinely. The experiment lasted for 12 weeks and the health of the mice was checked before each experiment to ensure that each mouse was healthy. After the experiment, the mice were sacrificed by cervical dislocation, blood was collected from the eye vein plexus, and the immune factors, testosterone, and progesterone were detected. At the same time, dissection was performed in a sterile studio, the organs were separated, the connective tissues around the organs were cut, and the hematoxylin-eosin (HE) staining method was used to make HE slices. The structure of each

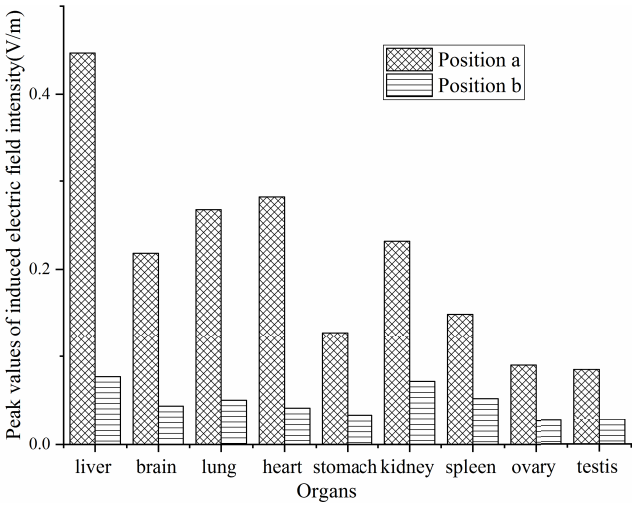

(a) Peak values of induced electric field intensity.

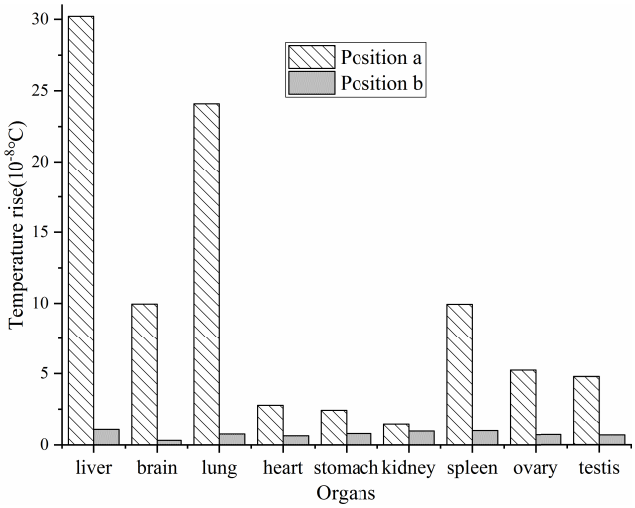

(b) Temperature rise.

FIGURE 11. Peak values of induced electric field intensity and temperature rise in different organs.

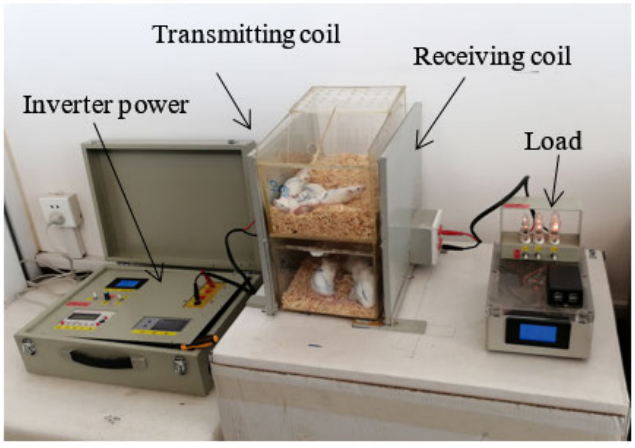

FIGURE 12. Experimental platform for the WPT system.

organ was observed under a light microscope at a magnification of 10 times.

The results of the immune factors are shown in Figure 13.

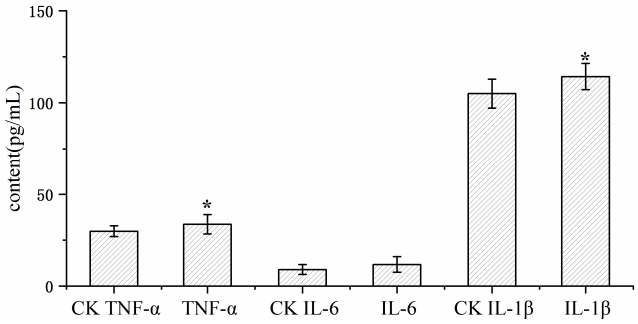

FIGURE 13. The content of immune factor.

As shown in Figure 13, the concentrations of tumor necrosis factor-α (TNF-α), interleukin-6 (IL-6), and interleukin-1β (IL-1β) in the serum of mice in the experimental group all increased. The significance indexes p of the contents of TNF-α and 1L-1β in the experimental group and the control group are less than 0.05. It shows that the exposure in the WPT system under this experimental condition will lead to an increase of TNF-α, IL-6 and IL-1β content in the serum of mice.

The content of progesterone and testosterone of mice are shown in figure 14.

As shown in Figure 14, the content of progesterone in the serum of female mice in the experimental group decreased, and the content of testosterone in the serum of male mice in the experimental group decreased, but the differences were not statistically significant ($p > 0.05$). The experimental results show that the WPT system can cause a downward trend in the content of the sex hormone of mice.

As shown in Figure 15, both the male and female mice in the experimental group had neatly arranged cells in their heart tissues, with clear structures and no obvious damage.

Male mice in the experimental group developed hepatocyte edema (4/5), as shown in Figure 16.

As shown in Figure 17, the interstitial substance of spleen cells in the female experimental group increased and the arrangement was loose (4/5). The male experimental group showed no obvious damage.

The ovaries of female mice in the experimental group shrank significantly and had polycystic changes (2/5), as shown in Figure 18. The testicular seminiferous tubule boundary membrane of the male mice in the experimental group was normal, the testicular cells had clear nucleoli, abundant cytoplasm, and most of the shapes remained unchanged, but the intercellular space increased, some cells became blurred borders and cell glands shrank (4/5), as shown in Figure 19.

IV. DISCUSSION

Comprehensive simulation data and experimental results show that under the experimental conditions, the peak values of induced electric field intensity and temperature rise of the mice are lower than the safety standards of the ICNIRP.

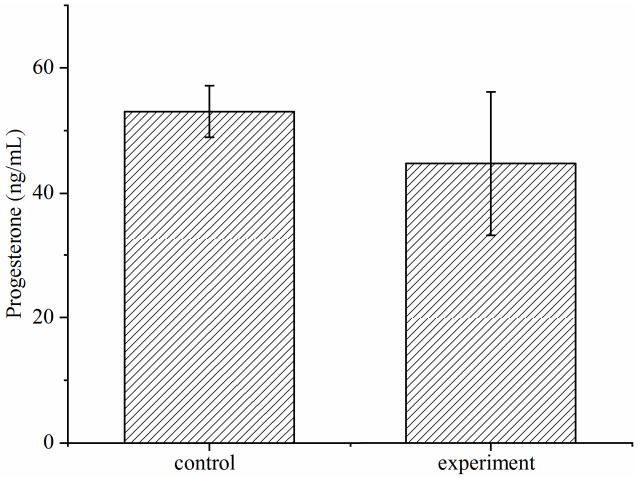

(a) Progesterone content.

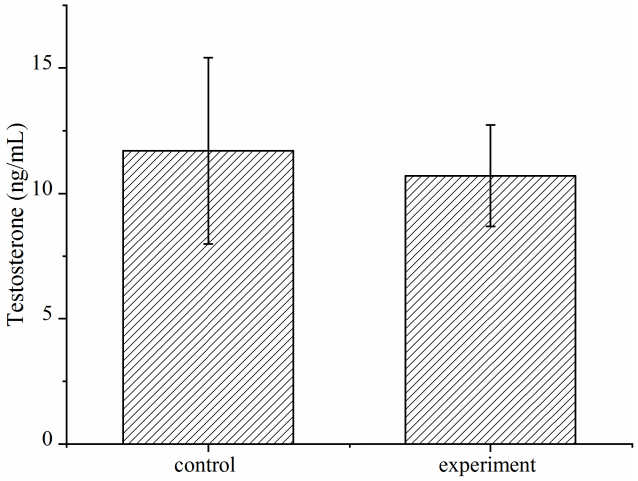

(b) Testosterone content.

FIGURE 14. Effects of the WPT system on sex hormones.

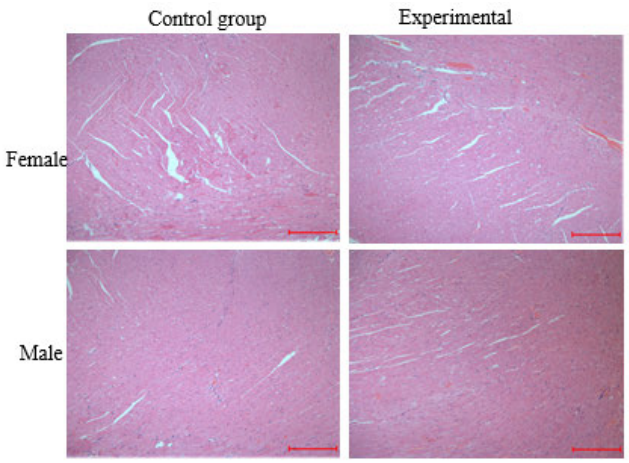

FIGURE 15. Effects of heart tissues of the WPT system (scalar bar with 100 μm).

After 12 weeks of exposure in the same condition, the heart tissue structure does not change, but the liver, spleen, ovary, and testes are affected. Therefore, it can be speculated that

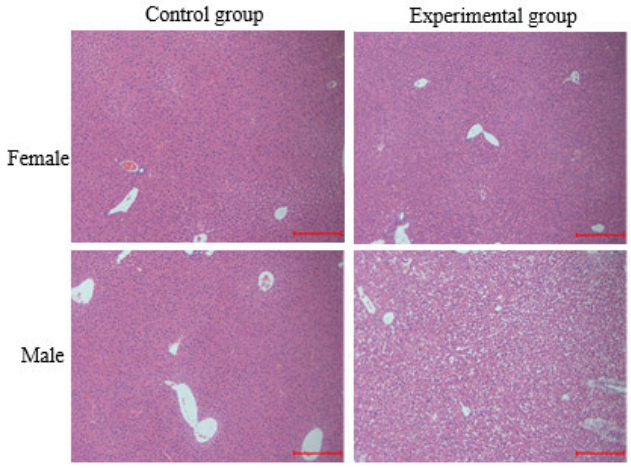

FIGURE 16. Effects of liver cells of the WPT system (scalar bar with 100 μm).

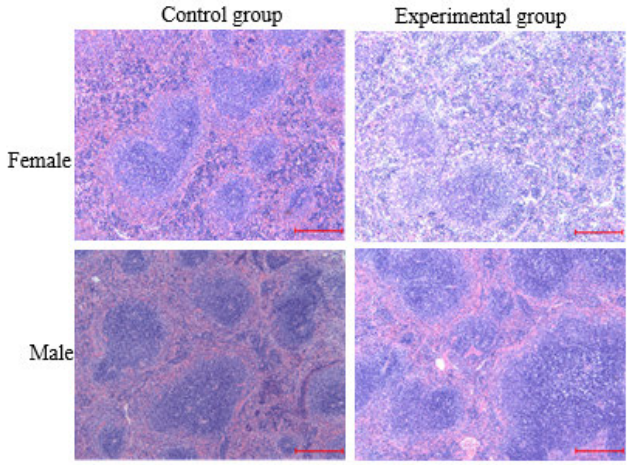

FIGURE 17. Effects of spleen cells of the WPT system (scalar bar with 100 μm).

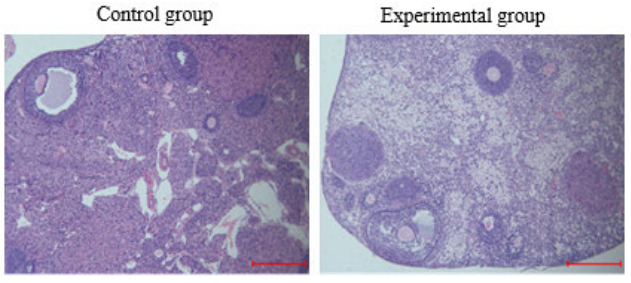

FIGURE 18. Effects of ovary cells of the WPT system(scalar bar with 100 μm).

although the induced electric field intensity of mouse organs is small, the cumulative effect of long-term radiation may still affect the health of mice.

When Li *et al.*studied the effect of iodine excess on immune function, it was found that more obvious morphological changes of the spleen in the mice with an active body's immune function [25]. Chauhan *et al.* [26] found that histological changes were observed in the spleen after whole-body microwave exposure, compared to the control group. Similar to the above results, in this work, it was found that the immune factor content of mice was significantly increased, the immune activity was enhanced, and morphological changes were observed. Above all, it is speculated that the morphological changes of the spleen of mice may be affected by the immune activity of the body.

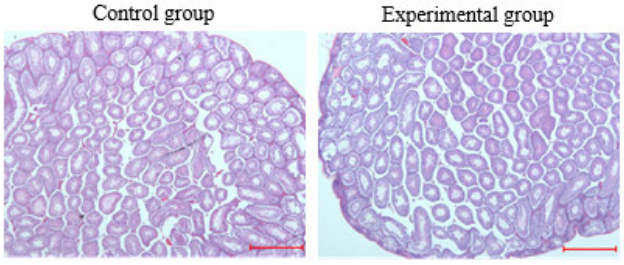

FIGURE 19. Effects of testis of the WPT system (scalar bar with 100 μm).

Liu exposed more than twenty mice to 900 MHz electromagnetic radiation with a special absorption rate of 0.66 ± 0.01 W/kg for 2 h/d. After 50 days, the percentage of apoptotic sperm cells in the exposure group was significantly increased and total antioxidant capacity in rat sperm was decreased greatly, which led to sperm cells decay rapidly [27]. Similar to the above results, when testing for sex hormones in this work, it was found that the content of male testosterone and female progesterone decreased, but the difference was not statistically significant ($p > 0.05$). The male testicular cell gap was increased, some cell borders were blurred and cell glands were shrunken. Besides, the female ovary was shrunken significantly and may show polycystic changes. Above all, it is speculated that the mechanism of electromagnetic radiation on the mouse reproductive system may be related to oxidative damage to germ cells.

The liver had the most effect in this experiment. Hepatic cell edema occurred and caused cell damage, which was consistent with the maximum peak value of the induced electric field intensity at the liver in the simulation results. Similar to the above results, Cevik *et al.* [28] found that long-term exposure to EMFs could cause inflammatory changes and apoptosis in liver of rats. It also explains that the simulation results are instructive to the experiment.

V. CONCLUSION

In this paper, a WPT system model and a mouse model are constructed at first. Based on this, the electromagnetic environment of the system is calculated, the peak values of induced electric field intensity and temperature changes of each organ when the mouse is in the system's electromagnetic field are analyzed too. The simulation results show that the peak value of induced electric field intensity of the liver is the largest, which is 1.43 V/m; the temperature rise of the kidney is the largest, which is 2.736×10^{-6}°C, and the calculation results of all organs are lower than the safety standards

formulated by the ICNIRP. The different cases of the mouse in the system are also simulated. And the results indicate that the shielding plate can effectively reduce the peak value of induced electric field intensity and temperature rise of the main organs. Then, a WPT system biosafety experimental platform is set up to analyze the changes in organ tissue structure, immune factors, and sex hormone content when mice are exposed to the WPT system. The experimental results show that there is no effect on the heart; the immune factor content of the mouse increases significantly, and the testosterone and progesterone content show a downward trend. It is speculated that the morphological changes of the spleen may be affected by the immune activity of the body, and the mechanism of electromagnetic radiation on the mouse reproductive system may be related to oxidative damage to germ cells. The liver is affected the most, which is consistent with the result that the peak value of induced electric field intensity of the liver is the largest. This study provides a theoretical basis for the security assessment of the WPT system.

REFERENCES

[1] L. Zhao, D. J. Thrimawithana, and U. K. Madawala, "Hybrid bidirectional wireless EV charging system tolerant to pad misalignment," *IEEE Trans. Ind. Electron.*, vol. 64, no. 9, pp. 7079–7086, Sep. 2017.

[2] S. Zhou and C. Chris Mi, "Multi-paralleled LCC reactive power compensation networks and their tuning method for electric vehicle dynamic wireless charging," *IEEE Trans. Ind. Electron.*, vol. 63, no. 10, pp. 6546–6556, Oct. 2016.

[3] R. Mai, Y. Chen, Y. Li, Y. Zhang, G. Cao, and Z. He, "Inductive power transfer for massive electric bicycles charging based on hybrid topology switching with a single inverter," *IEEE Trans. Power Electron.*, vol. 32, no. 8, pp. 5897–5906, Aug. 2017.

[4] T. Campi, S. Cruciani, F. Palandrani, V. De Santis, A. Hirata, and M. Feliziani, "Wireless power transfer charging system for AIMDs and pacemakers," *IEEE Trans. Microw. Theory Techn.*, vol. 64, no. 2, pp. 633–642, Feb. 2016.

[5] A. Kurs, A. Karalis, R. Moffatt, J. D. Joannopoulos, P. Fisher, and M. Soljacic, "Wireless power transfer via strongly coupled magnetic resonances," *Science*, vol. 317, no. 5834, pp. 83–86, Jul. 2007.

[6] D. O. Carpenter, "Human disease resulting from exposure to electromagnetic fields," *Rev. Environ. Health*, vol. 28, no. 4, pp. 159–172, 2013.

[7] S.-W. Park, "Dosimetry for resonance-based wireless power transfer charging of electric vehicles," *J. Electromagn. Eng. Sci.*, vol. 15, no. 3, pp. 129–133, Jul. 2015.

[8] F. Wen and X. Huang, "Human exposure to electromagnetic fields from Pparallel wireless power transfer systems," *Int. J. Environ. Res. Public Health*, vol. 14, no. 2, Feb. 2017, Art. no. 157.

[9] I. Laakso, S. Tsuchida, A. Hirata, and Y. Kamimura, "Evaluation of SAR in a human body model due to wireless power transmission in the 10 MHz band," *Phys. Med. Biol.*, vol. 57, no. 15, pp. 4991–5002, Aug. 2012.

[10] Q. Wang, W. Li, J. Kang, and Y. Wang, "Electromagnetic safety evaluation and protection methods for a wireless charging system in an electric vehicle," *IEEE Trans. Electromagn. Compat.*, vol. 61, no. 6, pp. 1913–1925, Dec. 2019.

[11] A. Christ, M. G. Douglas, J. M. Roman, E. B. Cooper, A. P. Sample, B. H. Waters, J. R. Smith, and N. Kuster, "Evaluation of wireless resonant power transfer systems with human electromagnetic exposure limits," *IEEE Trans. Electromagn. Compat.*, vol. 55, no. 2, pp. 265–274, Apr. 2013.

[12] K. Kim, J. Kim, H. Kim, J. Ahn, H. H. Park, and S. Ahn, "Evaluation of electromagnetic field radiation from wireless power transfer electric vehicle," in *Proc. Int. Symp. Antennas Propag. (ISAP)*, Okinawa, 2016, pp. 40–41.

[13] S. Park, "Evaluation of electromagnetic exposure during 85 kHz wireless power transfer for electric vehicles," *IEEE Trans. Magn.*, vol. 54, no. 1, pp. 1–8, Jan. 2018.

[14] A. Takei, K. Murotani, S.-I. Sugimoto, M. Ogino, and H. Kawai, "Performance evaluation of parallel finite element electromagnetic field analysis using numerical human models in HPCI," in *Proc. IEEE Conf. Electromagn. Field Comput. (CEFC)*, Miami, FL, USA, Nov. 2016, pp. 127–140.

[15] S. Greenland and L. Kheifets, "Designs and analyses for exploring the relationship of magnetic fields to childhood leukaemia: A pilot project for the danish national birth cohort," *Scandin. J. Public Health*, vol. 37, no. 1, pp. 83–92, Jan. 2009.

[16] L. Kheifets, A. Ahlbom, C. M. Crespi, G. Draper, J. Hagihara, R. M. Lowenthal, G. Mezei, S. Oksuzyan, J. Schüz, J. Swanson, A. Tittarelli, M. Vinceti, and V. Wunsch Filho, "Pooled analysis of recent studies on magnetic fields and childhood leukaemia," *Brit. J. Cancer*, vol. 103, no. 7, pp. 1128–1135, Sep. 2010.

[17] C. Fernández, A. A. de Salles, M. E. Sears, R. D. Morris, and D. L. Davis, "Absorption of wireless radiation in the child versus adult brain and eye from cell phone conversation or virtual reality," *Environ. Res.*, vol. 167, pp. 694–699, Nov. 2018.

[18] S. Ohtani, A. Ushiyama, M. Maeda, Y. Ogasawara, J. Wang, N. Kunugita, and K. Ishii, "The effects of radio-frequency electromagnetic fields on t cell function during development," *J. Radiat. Res.*, vol. 56, no. 3, pp. 467–474, May 2015.

[19] S. Gabriel, R. W. Lau, and C. Gabriel, "The dielectric properties of biological tissues: II. Measurements in the frequency range 10 Hz to 20 GHz," *Phys. Med. Biol.*, vol. 41, no. 11, pp. 2251–2269, 1996.

[20] International Commission on Non-Ionizing Radiation Protection, "Guidelines for limiting exposure to time-varying electric and magnetic fields (1 Hz to 100 kHz)," *Health Phys.*, vol. 99, no. 6, pp. 818–836, 2010.

[21] J. Zhang, R. Y. Peng, S. M. Wang, Y. B. Gao, W. Song, X. Li, J. Dong, and L. Zhao, "Effects of long-term low doses of microwave radiation on biochemical indexes of serum and the myocardial histological structure in rats," *Mil. Med. Sci.*, vol. 35, no. 5, pp. 351–354, 2011.

[22] L. Wang, T. Yang, J. Zhao, and G. Z. Xu, "Effects of electromagnetic field on immune logical traits of mice in wireless charging of electric vehicles," *Chin. J. Radio.*, vol. 34, no. 4, pp. 492–498, 2019.

[23] H. Mahaki, H. Tanzadehpanah, N. Jabarivasal, K. Sardanian, and A. Zamani, "A review on the effects of extremely low frequency electromagnetic field (ELF-EMF) on cytokines of innate and adaptive immunity," *Electromagn. Biol. Med.*, vol. 38, no. 1, pp. 84–95, Jan. 2019.

[24] H. Y. Dong, X. J. Hu, R. Y. Peng, L. F. Wang, L. Chen, and Y. X. Li, "Research on the change of structure and blood-air barrier permeability of rat lung induced by microwave exposure," *J. Prevention Med. Chin. Peopl. Liber. Army*, vol. 35, no. 10, pp. 1206–1208, 2017.

[25] J. R. Li, L. N. Zheng, S. Z. Wang, N. Hu, and H. Liu, "The histological study on mice spleen with iodine excess," *Anat. Res.*, no. 5, pp. 506–508 and 511, Sep. 2007.

[26] P. Chauhan, H. N. Verma, R. Sisodia, and K. K. Kesari, "Microwave radiation (2.45 GHz)-induced oxidative stress: Whole-body exposure effect on histopathology of Wistar rats," *Electromagn. Biol. Med.*, vol. 36, no. 1, pp. 20–30, 2017.

[27] Q. Liu, T. Si, X. Xu, F. Liang, L. Wang, and S. Pan, "Electromagnetic radiation at 900 MHz induces sperm apoptosis through Bcl-2, Bax and Caspase-3 signaling pathways in rats," *Reproductive Health*, vol. 12, no. 1, pp. 1–9, Aug. 2015.

[28] A. Cevik, M. Aydin, A. M. Apaydin, and M. Yuksel, "Pathological and immunohistochemical effects of electromagnetic fields on rat liver," *Indian J. Animal Res.*, vol. 51, no. 6, pp. 1134–1137, Nov. 2017.

JUN ZHAO received the Ph.D. degree in electrical engineering from the Hebei University of Technology, Tianjin, in 2013. She is currently working as a Senior Experimenter at the Hebei University of Technology. Her current research interests include wireless power transmission and electromagnetic biological effects.

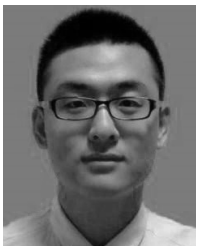

ZHIJUN WU received the B.S. degree in electrical engineering from the Qingdao University of Technology, in 2018. He is currently pursuing the M.S. degree with the Hebei University of Technology. His current research interests include wireless power transmission and electromagnetic biological effects.

TING YANG received the B.S. degree in biomedical engineering from the City College, Hebei University of Technology, Tianjin, China, in 2017, and the M.S. degree in biomedical engineering from the Hebei University of Technology, in 2020. Her current research interest includes electromagnetic biological effects.

YIHANG ZHAO received the B.S. degree in electrical engineering from Handan University, in 2019. He is currently pursuing the M.S. degree with the Hebei University of Technology. His current research interests include wireless power transmission and electromagnetic biological effects.

LEI WANG received the Ph.D. degree in electrical engineering from the Hebei University of Technology, Tianjin, in 2019. He is working with the Institute of Biomedical Engineering, Chinese Academy of Medical Sciences and Peking Union Medical College. His research interest includes electromagnetic biological effects.